

10-25-2016

Giant reversible inverse magnetocaloric effects in Ni₅₀Mn₃₅In₁₅ Heusler alloys

Abdiel Quetz
Southern Illinois University Carbondale

Yury S. Koshkid'Ko
VSB – Technical University of Ostrava

Ivan Titov
Lomonosov Moscow State University

Igor Rodionov
Lomonosov Moscow State University

Sudip Pandey
Southern Illinois University Carbondale

See next page for additional authors

Follow this and additional works at: https://digitalcommons.lsu.edu/physics_astronomy_pubs

Recommended Citation

Quetz, A., Koshkid'Ko, Y., Titov, I., Rodionov, I., Pandey, S., Aryal, A., Ibarra-Gaytan, P., Prudnikov, V., Granovsky, A., Dubenko, I., Samanta, T., Cwik, J., Llamazares, J., Stadler, S., Lähderanta, E., & Ali, N. (2016). Giant reversible inverse magnetocaloric effects in Ni₅₀Mn₃₅In₁₅ Heusler alloys. *Journal of Alloys and Compounds*, 683, 139-142. <https://doi.org/10.1016/j.jallcom.2016.05.106>

This Article is brought to you for free and open access by the Department of Physics & Astronomy at LSU Digital Commons. It has been accepted for inclusion in Faculty Publications by an authorized administrator of LSU Digital Commons. For more information, please contact ir@lsu.edu.

Authors

Abdiel Quetz, Yury S. Koshkid'Ko, Ivan Titov, Igor Rodionov, Sudip Pandey, Anil Aryal, Pablo J. Ibarra-Gaytan, Valery Prudnikov, Alexander Granovsky, Igor Dubenko, Tapas Samanta, J. Cwik, José L.S. Llamazares, Shane Stadler, E. Lähderanta, and Naushad Ali

Giant Reversible Inverse Magnetocaloric Effects in Ni₅₀Mn₃₅In₁₅ Heusler alloys

Abdiel Quetz^{1a)}, Yury S. Koshkid'ko^{2,3}, Ivan Titov⁴, Igor Rodionov⁴, Sudip Pandey¹, Anil Aryal¹, Pablo J. Ibarra-Gaytan⁵, Valery Prudnikov⁴, Alexander Granovsky⁴, Igor Dubenko¹, Tapas Samanta⁶, J. Cwik³, José L. S. Llamazares⁵, Shane Stadler⁶, E. Lähderanta⁷, and Naushad Ali¹

¹Department of Physics, Southern Illinois University, Carbondale, Illinois 62901, USA

²VSB-Technical University of Ostrava, Ostrava-Poruba 708 33, Czech Republic

³International Laboratory of High Magnetic Fields and Low Temperatures, Wrocław 53-421, Poland

⁴Faculty of Physics, Lomonosov Moscow State University, Vorob'evy Gory, 119991 Moscow, Russia

⁵Instituto Potosino de Investigación Científica y Tecnológica, Camino a la Presa San José 2055, Col. Lomas 4^a, San Luis Potosí S.L.P. 78216, Mexico

⁶Department of Physics & Astronomy, Louisiana State University, Baton Rouge, Louisiana 70803, USA

⁷Lappeenranta University of Technology, Lappeenranta 53851, Finland

Abstract

The magnetic properties and reversibility of the magnetocaloric effect of Ni₅₀Mn₃₅In₁₅ have been studied in the vicinity of the phase transition using magnetization and direct adiabatic temperature change (ΔT_{ad}) measurements in magnetic fields up to 14 T. The magnetostructural phase transitions (MSTs) between a martensitic phase (MP) with low magnetization (paramagnetic or antiferromagnetic) and a nearly ferromagnetic austenitic phase were detected from thermomagnetic curves, $M(T,H)$, at the applied magnetic fields up to 5 T. The MST temperature was found to be nearly independent of magnetic field for $H < 5$ T, and shifted to lower temperature with the further increase of magnetic field to 14 T. A large and nearly reversible inverse magnetocaloric effect (MCE) with $\Delta T_{ad} \sim -11$ K for a magnetic field change of $\Delta H = 14$ T was observed in the vicinity of the MST. The irreversibility of ΔT_{ad} was found to be 1 K. A direct ΔT_{ad} of +7 K for $\Delta H = 14$ T was detected at the second order ferromagnetic-paramagnetic phase transition. The obtained results have been discussed in terms of the suppression of antiferromagnetic correlations with the application of a strong magnetic field, and a reversibility of the initial magnetic state of the MP with applied magnetic field when the MST coincides with T_C .

^{a)} Author to whom correspondence should be addressed. Electronic mail: anorve2002@yahoo.com

Keywords: Heusler Alloys, Magnetostructural Phase Transition, Giant MCE materials

I. INTRODUCTION

The off-stoichiometric Ni-Mn-In based Heusler alloys with compositions near $\text{Ni}_{50}\text{Mn}_{35}\text{In}_{15}$ undergo first order temperature-induced structural/martensitic transitions at $T = T_M$ near room temperature. The magnetic states of the high temperature austenitic phase (AP) and low temperature martensitic phase (MP) were found to be different in these compounds near T_M . Thus, the martensitic transition can be induced by external magnetic field and results in a jump-like variation in the magnetization and magneto-responsive properties, i.e., it undergoes a magnetostructural phase transition (MST). Magnetic transitions of paramagnetic (PM) MP to a PM austenitic phase, low-magnetization state (LM, paramagnetic or antiferromagnetic) MP to ferromagnetic AP, and ferromagnetic MP – paramagnetic AP types have been reported at MSTs in Ref. [1-4]. Normal and inverse magnetocaloric effects (MCEs), exchange bias, temperature- and field- induced phase transitions, giant magnetoresistance, and giant Hall effects have been observed in systems based on $\text{Ni}_{50}\text{Mn}_{50-x}\text{In}_x$ in the vicinity of $x=15$ [5-7]. Consequently, these materials are attractive candidates for multifunctional devices, where magnetic and structural characteristics may be manipulated by applied magnetic fields. Since, the magnetocaloric effect results from magnetization changes, remarkable MCE values and time dependency of adiabatic temperature changes have already been reported for these alloys [1, 5-14] and, in Ref. [15], respectively. An important MCE parameter that characterizes the applicability of materials for magnetic refrigeration is the adiabatic temperature change (ΔT_{ad}). However, for practical applications besides high values of ΔT_{ad} its reversibility in cycling magnetic fields is of primary importance.

The ΔT_{ad} of alloys based on $\text{Ni}_{50}\text{Mn}_{50-x}\text{In}_x$ with $x \sim 15$ have been studied in the vicinity of the phase transitions using direct measurements in Ref. [4-13]. The largest measured changes were $\Delta T_{\text{ad}} = -2$ K and 2 K near the martensitic (first order) and ferromagnetic (second order, at T_C) transitions for $\Delta H = 1.8$ T, respectively [7, 11]. Our preliminary results showed that these values can be significantly enhanced up to ~ 11 K near the MST in strong magnetic fields (up to

14 T) for the first magnetization cycle [12, 13]. A large ΔT_{ad} of -6.2 K ($\Delta H = 1.9$ T) was reported in Ref. [16] for a $Ni_{45.2}Mn_{36.7}In_{13}Co_5$ alloy at the MST. However, the initial value of $\Delta T_{ad} = -6.2$ K observed for the first magnetization cycle was found to drop to about -2 K for the second and subsequent cycles. Thus, the irreversibility of ΔT_{ad} was found to be about 70%. The ΔT_{ad} of -12.8 K was measured for $Ni_{45}Co_5Mn_{36.7}In_{13.3}$ for the first cycle of a pulsed magnetic field ($\Delta H=15$ T) in Ref. [16] but the reversibility was not demonstrated.

In the manuscript, we report the dependence of the MST temperature of $Ni_{50}Mn_{35}In_{15}$ on magnetic field, and the associated reversibility of ΔT_{ad} . A nearly reversible ΔT_{ad} of about -10 K (1 K less for the subsequent cycles) was observed in the vicinity of the MST. The observed behavior has been attributed to specific features of the magnetic states of both the MP and AP close to the MST connected with strong antiferromagnetic correlations and the proximity to long-range ferromagnetic order.

II. EXPERIMENTAL DETAILS

The $Ni_{50}Mn_{35}In_{15}$ (nominal composition) compounds were fabricated by conventional arc-melting in a high-purity argon atmosphere using 4N purity elements and were subsequently annealed in high vacuum ($\sim 10^{-4}$ Torr) for 24 hours at 850 °C. The phase purities of the compounds were confirmed by x-ray powder diffraction at room temperature using CuK α radiation. Thermomagnetic curves $M(H,T)$ have been acquired using a superconducting quantum interference device (SQUID) magnetometer (by Quantum Design, USA) and by a Quantum Design PPMS-9T platform in fields up to $H = 5$ T and 9 T, respectively, in a temperature interval of 5-400 K. Magnetization (M) was measured in the temperature range (4.2–300) K by the vibrating magnetometer method. As the source of the magnetic field, an Oxford Instruments superconducting solenoid was used, producing magnetic fields up to 14 T. Direct measurements of ΔT_{AD} under applied magnetic fields up to 14 T were done using a Bitters electromagnet and employing the “extraction/insertion” method (see for details of this set-up in Ref. [13]). The time

of “extraction/insertion” from maximum to zero magnetic fields regions was 2.5 s. Direct measurements of ΔT_{AD} at $\Delta H=1.8$ T have been done using an adiabatic magnetocalorimeter (MagEqMMS 801) in a temperature range of 250 K–350 K. The external magnetic fields were ramped at a rate of up to 2.0 T/s during the measurements. The $\text{Ni}_{50}\text{Mn}_{35}\text{In}_{15}$ samples were heated to 380 K prior to the measurements. The temperature dependences of the magnetization, $M(T)$, at applied magnetic field (H) were carried out during heating after the samples were cooled from 380 K to 10 K at zero magnetic field (ZFC), and during a field-cooling cycle (FCC).

III. RESULTS AND DISCUSSION

A mixture of high temperature cubic AP and low temperature MP was observed in the room-temperature x-ray diffraction patterns. The MP and AP were identified as orthorhombic and cubic, respectively (see Fig. 1). The co-existence of AP and MP crystal phases results from the austenitic and martensitic phase temperature hysteresis originating from the temperature-induced, first order structural transition.

The behavior of the magnetization curves was found to be different at low and high magnetic fields. The inverse (at T_A) and direct (at T_M) martensitic transformations, and the FM-PM (at T_C), are clearly identified from the jump-like changes in magnetization and inflection points of the $M(T)$ curves, respectively, at magnetic fields $H > 2$ T (see Fig. 2). However, at low magnetic fields (see for $H=0.005$ and 0.01 T in Fig. 2), no features characteristic of the FM-PM transition were observed. The obtained maximum values of magnetization of about 0.3 emu/g (on heating) and 1.2 emu/g (on cooling) of the austenitic phase in the vicinity of the martensitic transition (MT) are comparable to that of 0.6 emu/g observed above the structural phase transition from a paramagnetic martensitic state to a paramagnetic austenitic state in $\text{Ni}_{50}\text{Mn}_{36.5}\text{In}_{13.5}$ Heusler alloys [14] at the same magnetic field of 0.01 T. Taking into account the small value of magnetization of the AP of about 1.25/0.6 emu/g at $H= 0.01$ T (see Fig. 2), one can conclude that the AP phase remains in the paramagnetic (or “quasiferromagnetic”) state at low magnetic fields for all temperatures above T_M , and therefore the hypothetical T_C of the AP is

slightly below T_M . The martensitic transformation temperature, T_A and T_M , are nearly constant at magnetic fields less than 5 T, and decreases by about 28 K at $H=14$ T (see Fig. 3). In our case the MST is unconventional, namely, at low magnetic fields (less than 2 T), the MST results in a transition from a low magnetization MP to paramagnetic AP, which state is very close to long-range ferromagnetic order, the subsequent increase in applied magnetic field promotes the FM ordering of AP, and therefore the decrease in the martensitic transition temperatures. Apparently, in such a case when the MST occurs between two “paramagnetic“ phases one can expect the reversibility for MCE, like in the case of MCE in paramagnetic salts at low temperatures. The MST temperature can be described as a quadratic function of applied magnetic field (see Fig. 3).

An inverse ΔT_{AD} of about -1 K (for $\Delta H= 1.8$ T) and -11 K (for $\Delta H= 14$ T), and the ΔT_{AD} of 1 K (for $\Delta H= 1.8$ T) and about 7 K (for $\Delta H= 14$ T) were observed at the first order MST, and at the second order magnetic transition at T_C , respectively (see Fig. 4). Thus, the application of a strong magnetic field ($\Delta H= 14$ T) results in a giant increase in ΔT_{AD} by about an order of magnitude for both the first and second order transitions. Moreover, nearly reversible changes in ΔT_{AD} of -10.4 K and -9.4 K were observed for the first and subsequent magnetization cycles at the MST for $\Delta H = 14$ T (see Fig. 5).

The ΔT_{AD} at the second order transitions depends on the applied magnetic field as $\Delta T_{AD} \sim \Delta H^{2/3}$ (see, for example, in Refs. [11]). Therefore, the increase of ΔH from 1.8 to 14 T should provide about a four-fold increase in ΔT_{AD} . However, the observed increase in ΔT_{AD} is more than six-fold (see Fig. 4 for the second-order transition). Such a discrepancy can be explained by the magnetic inhomogeneity of the AP in the vicinity of the MST. The inhomogeneity results in antiferromagnetic correlations or antiferromagnetic “pinning” of the magnetization originating from antiferromagnetic coupling of the moments of Mn in In atomic positions (anti-site Mn moments) relative to properly located Mn moments on Mn atomic sites in off-stoichiometry Heusler alloys (for details see the Ref. [17-20]). Thus, the antiferromagnetic correlations interfere with the ferromagnetic ordering, and are responsible for the virtually constant T_M/T_A in

the low and intermediate magnetic field regions ($H < 5$ T). In contrast, the strong magnetic fields suppress the antiferromagnetic correlations, thereby providing the extra contribution to the MCE. It can be clearly seen in Fig. 4 that the MCE is nearly constant with respect to temperature ($\Delta T \sim 1$ K) below MST. A temperature hysteresis of 2.5 K has been observed for ΔT_{AD} in the vicinity of the MST.

The adiabatic temperature changes induced by the external magnetic field changes in the vicinity of the magnetostructural transition ($T=315$ K) as function of the time for several cycles of magnetic field application are shown in Figure 5. From the first and second magnetization cycles, a giant inverse ΔT_{AD} of -10.4 K and -9.4 K were measured, respectively, at temperatures below and close to T_A (see Fig. 5). The observed irreversibility is about seven times smaller compared to that reported for the Ni-Mn-In-5% Co alloy [16]. The difference is most likely related to the difference in the magnetic states of the austenitic phases in the vicinity of the martensitic transition. It has been reported that, in the case of the Ni-Mn-In-5% Co alloy, the phase transition temperatures are separated and the martensitic transformation takes place well below the T_C of austenitic phase. The low magnetization phase transforms to the strong ferromagnetic austenitic phase ($M \sim 100$ emu/g, for $H=2$ T) at the temperature of the inverse martensitic transition [16]. In contrast, the MST from low magnetization to the “paramagnetic” austenitic phase ($M \sim 20$ emu/g, at $H=2$ T) was observed for $Ni_{50}Mn_{35}In_{15}$. The low magnetization state is characterized by structural-magnetic heterogeneity originating from the austenite/martensite temperature hysteresis and described, based on magnetization behavior, as an antiferromagnetic or paramagnetic state (see Ref. [6] and references therein). Therefore, the low magnetization state in the vicinity and below the temperature of the martensitic transformation can be considered as austenitic paramagnetic inclusions in a martensitic “matrix”. If the martensitic transformation occurs above the T_C of the AP the ferromagnetic interaction in AP is weak and can provide only short-range ferromagnetic order. As a result the AP phase remains paramagnetic but its magnetization can be strongly enhanced in applied magnetic fields,

therefore, a reversible magnetization process can be expected. Consequently, a nearly reversible ΔT_{AD} was observed for $Ni_{50}Mn_{35}In_{15}$ at temperatures near and below T_A .

IV. CONCLUSION

A nearly reversible ΔT_{ad} of -10.4 K (-9.4 K for the second and subsequent cycles) was observed in the close proximity to the MST for $Ni_{50}Mn_{35}In_{15}$. The reversibility of the MCE has been explained by a nearly “reversible” magnetic state of the MP with applied magnetic field when the MST coexists with the T_C .

ACKNOWLEDGMENTS

This work was supported by the Office of Basic Energy Sciences, Material Science Division of the U.S. Department of Energy (DOE Grant No. DE-FG02-06ER46291 (SIU), and DE-FG02-13ER46946 (LSU)). The authors from Lomonosov Moscow State University acknowledge support from the Russian Foundation for Basic Research (Grant No. 15-02-01976 and 16-32-00460 (Rodionov)). J. L. Sánchez Llamazares acknowledges the support received from CONACYT, Mexico (Grant Nos. 157541, and 156932), and Laboratorio Nacional de Investigaciones en Nanociencias y Nanotecnología (LINAN, IPICYT).

REFERENCES

- [1] I. Dubenko, N. Ali, S. Stadler, A. Zhukov, V. Zhukova, B. Hernando, V. Prida, V. Prudnikov, E. Ganshina, and A. Granovsky, Magnetic, Magnetocaloric, Magnetotransport, And Magneto-Optical Properties Of Ni-Mn-In – Based Heusler Alloys: Bulk, Ribbons, And Microwires, in Novel Functional Magnetic Materials, Springer Series in Materials Science, Ed. A. Zhukov, (2016) p.p. 41-82
- [2] T Krenke, M. Acet, E. F. Wassermann, X. Moya, L. Man˜osa, and A. Planes, Phys. Rev. B **73**, 174413 (2006).
- [3] Krenke, E. Duman, M. Acet, E. Eberhard, F. Wassermann, X. Moya, L. Manosa, and A. Planes, Phys. Rev. B **75**, 104414 (2007).
- [4] A. P. Kazakov, V. N. Prudnikov, A. B. Granovsky, A. P. Zhukov, J. Gonzalez, I. Dubenko, A. K. Pathak, S. Stadler, N. Ali, Appl. Phys. Lett. **98** 131911 (2011).
- [5] I. Dubenko, M. Khan, A. K. Pathak, B. R. Gautam, S. Stadler, and N. Ali, J. Magn. Magn. Mat. **321** (2009) 754-757.
- [6] I. Dubenko, T. Samanta, A. Kumar Pathak, A. Kazakov, V. Prudnikov, S. Stadler, A. Granovsky, A. Zhukov and N. Ali, J. Magn. Mag. Mat. **324** (2012), pp. 3530 – 3534.
- [7] I. Dubenko, A. Quetz, S. Pandey, A. Aryal, M. Eubank, I. Rodionov, V. Prudnikov, A. Granovsky, E. Lahderanta, T. Samanta, A. Saleheen, S. Stadler, N. Ali, J. Magn. Mag. Mat, **383** (2015) 186–189.
- [8] Dubenko, I., Samanta, T., Quetz, A., Kazakov, A., Rodionov, I., Mettus, D., Prudnikov, V., Stadler, S., Adams, P., Prestigiacomo, J., Granovsky, A., Zhukov, A., Ali, N., *Appl. Phys. Lett.* **100** (2012) 192402-4.
- [9] I. Dubenko, T. Samanta, A. Quetz, A. Kazakov, I. Rodionov, D. Mettus, V. Prudnikov, S. Stadler, P.W. Adams, J. Prestigiacomo, A. Granovsky, A. Zhukov, and N. Ali, *IEEE Trans. Magn.*, **48** (2012) 3738-3741.

- [10] Kazakov, A. P., Prudnikov, V. N., Granovsky, A. B., Zhukov, A. P., Gonzalez, J., Dubenko, I., Pathak, A. K., Stadler S., Ali, N., *Appl. Phys. Lett.*, **98**, 2011, 131911-3.
- [11] Kazakov, A., Prudnikov, V., Granovsky, A., Perov, N., Dubenko, I., Pathak, A. K., Samanta, T., Stadler, S., Ali, N., Zhukov, A., Ilyin, M., Gonzalez, J., *Journal of Nanoscience and Nanotechnology*, **12**, 2012, 7426-7431.
- [12] I. D. Rodionov, Yu. S. Koshkid'ko, J. Cwik, A. Quetz, S. Pandey, A. Aryal, I. S. Dubenko, S. Stadler, N. Ali, I. S. Titov, M. Blinov, M. V. Prudnikova, V. N. Prudnikov, E. Lahderanta, and A. B. Granovskii, *JETP Letters*, , **101**, 2015, 385–389.
- [13] Igor D. Rodionov, Yurii S. Koshkid'ko, Jacek Cwik, Abdiel Quetz, Sudip Pandey, Anil Aryala, Igor S. Dubenko, Shane Stadler, Naushad Ali, Ivan S. Titov, Mikhail Blinov, Valery N. Prudnikov, Erkki Lahderanta, Ivan Zakharchuk, and Alexander B. Granovsky, *Physics Procedia* **75**, 1353-1359 (2015).
- [14] A. K. Pathak, I. Dubenko, C. Pueblo, S. Stadler, and N. Ali, *Appl. Phys. Lett.* **96** 172503 (2010).
- [15] T. Gottschall, K. P. Skokov, F. Scheibel, M. Acet, M. Ghorbani Zavareh, Y. Skourski, J. Wosnitza, M. Farle, and O. Gutfleisch, *Physical Review Applied* **5**, 024013 (2016).
- [16] J. Liu, T. Gottschall, K.P. Skokov, and O. Gutfleisch, *Nature Materials* **11**, 620 (2012).
- [17] T. Kihara, X. Xu, W. Ito, R. Kainuma, M. Tokunaga, *Phys. Rev. B* **90**, 214409 (2014).
- [18] C.V. Stager, C.C.M. Campbell, *Can. J. Phys.* **56** (1978) 674.
- [19] J. Enkovaara, O. Heczko, A. Ayuela, R. M. Nieminen, *Phys.Rev. B* **67** (2003) 212405.
- [20] P. J. Shamberger, F. S. Ohuchi, *Phys.Rev. B* **67** (2009) 144407

Figures and Figure Captions

Fig. 1: Powder XRD patterns of $\text{Ni}_{50}\text{Mn}_{35}\text{In}_{15}$ at room temperature.

Fig. 2 ZFC and FCC $M(T)$ curves for different applied magnetic fields. T_M and T_A are the temperatures of the direct and inverse martensitic transformations.

Fig. 3 The field dependence of the martensitic transition temperatures.

Fig.4 (a) Temperature dependence of the adiabatic temperature change ΔT_{ad} in $\text{Ni}_{50}\text{Mn}_{35}\text{In}_{15}$ alloys in an applied magnetic field of 14 T (inset shows the same for $H = 1.8$ T, the data were taken from Ref. [12]) in the vicinity of the martensitic transformation; (b) The corresponding curves for a narrow temperature range in the area of temperature hysteresis.

Fig.5 The adiabatic temperature (left panel) and external magnetic field (right panel) changes as a function of time obtained for a maximum value of $\Delta H = 14$ T at the first and subsequent magnetization cycles at $T = 315$ K.

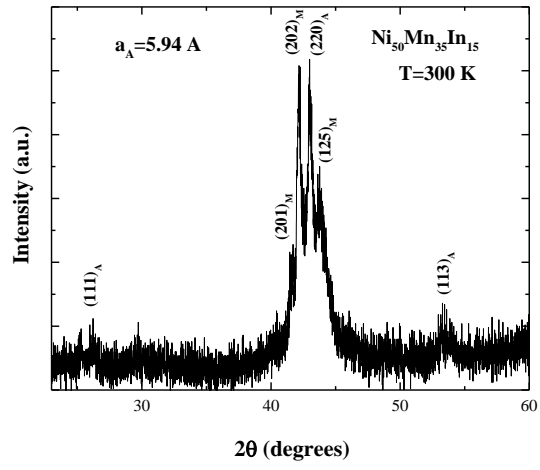


Fig. 1: Powder XRD patterns of $\text{Ni}_{50}\text{Mn}_{35}\text{In}_{15}$ at room temperature.

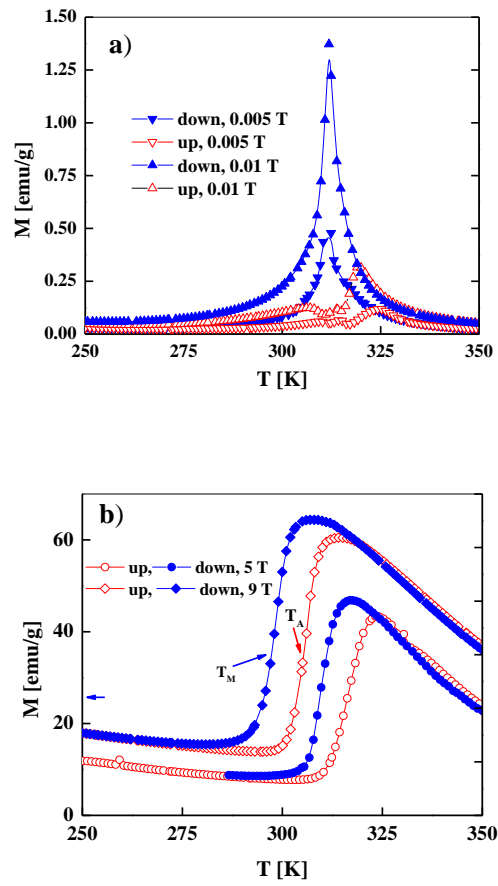


Fig. 2 ZFC and FCC $M(T)$ curves for (a) low applied magnetic fields and (b) strong magnetic fields. T_M and T_A are the temperatures of the direct and inverse martensitic transformations.

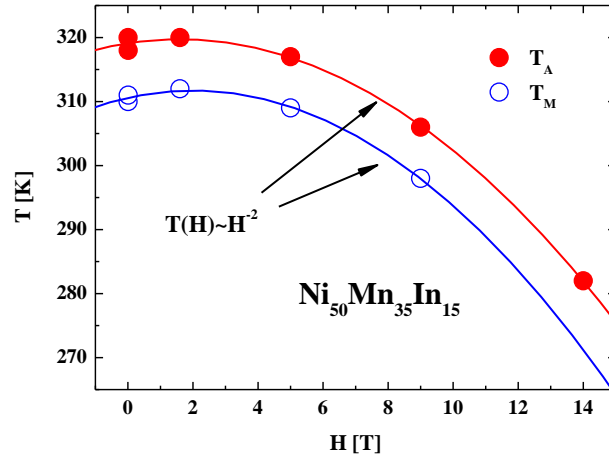


Fig. 3 The field dependence of the martensitic transition temperatures.

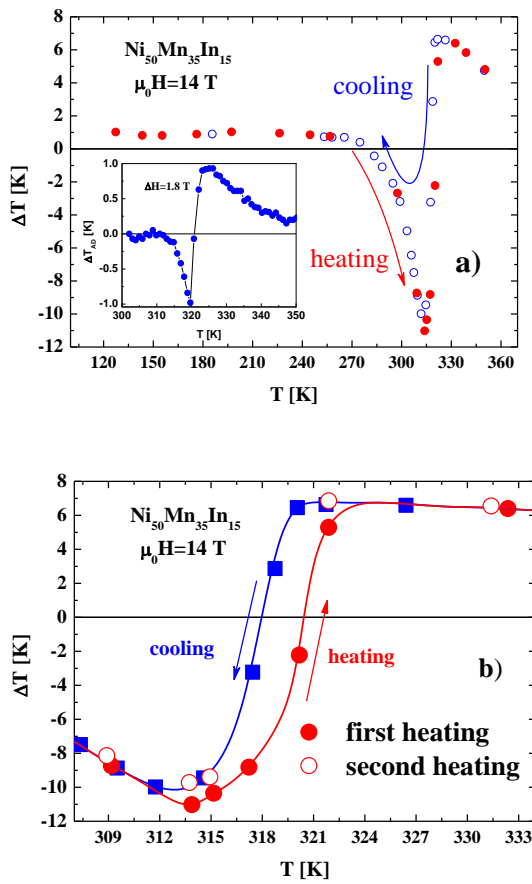


Fig.4 (a) Temperature dependence of the adiabatic temperature change ΔT_{ad} in $\text{Ni}_{50}\text{Mn}_{35}\text{In}_{15}$ alloys in an applied magnetic field of 14 T (inset shows the same for $H = 1.8$ T, the data were taken from Ref. [12]) in the vicinity of the martensitic transformation; (b) The corresponding curves for a narrow temperature range in the area of temperature hysteresis.

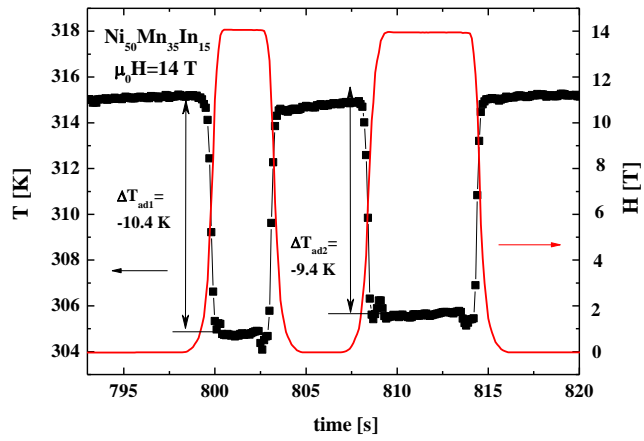


Fig.5 The adiabatic temperature (left panel) and external magnetic field (right panel) changes as a function of time obtained for a maximum value of $\Delta H=14$ T at the first and subsequent magnetization cycles at $T = 315$ K.